DRAWING EARLY-BIRD TICKETS: TOWARDS MORE EFFICIENT TRAINING OF DEEP NETWORKS

Anonymous authors
Paper under double-blind review

ABSTRACT

(Frankle & Carbin, 2019) shows that there exist *winning tickets* (small but critical subnetworks) for dense, randomly initialized networks, that can be trained alone to achieve comparable accuracies to the latter in a similar number of iterations. However, the identification of these winning tickets still requires the costly train-prune-retrain process, limiting their practical benefits. In this paper, we discover for the first time that the **winning tickets can be identified at the very early training stage**, which we term as **early-bird (EB)** tickets, via low-cost training schemes (e.g., early stopping, low-precision training) at large learning rates. Our finding of EB tickets is consistent with recently reported observations that the key connectivity patterns of neural networks emerge early. Furthermore, we propose a mask distance metric that can be used to identify EB tickets with low computational overhead, without needing to know the true winning tickets that emerge after the full training. Finally, we leverage the existence of EB tickets and the proposed mask distance to develop efficient training methods, which are achieved by first identifying EB tickets via low-cost schemes, and then continuing to train merely the EB tickets towards the target accuracy. Experiments based on various deep networks and datasets validate: 1) the existence of EB tickets, and the effectiveness of mask distance in efficiently identifying them; and 2) that the proposed efficient training via EB tickets can achieve up to **4.7**$\times$ **energy savings** while maintaining comparable or even better accuracy, demonstrating a promising and easily adopted method for tackling cost-prohibitive deep network training.

1 INTRODUCTION

The recent record-breaking predictive performance achieved by deep neural networks (DNNs) motivates a tremendously growing demand to bring DNN-powered intelligence into numerous applications. However, the excellent performance of modern DNNs comes at an often prohibitive training cost due to the required vast volume of training data and model parameters. As an illustrative example of the computational complexity of DNN training, one forward pass of the ResNet50 (He et al. (2016a)) model requires 4 GFLOPs (FLOPs: floating point operations per second) of computations and training requires 10^{18} FLOPs, which takes 14 days on one state-of-the-art NVIDIA M40 GPU (You et al. (2018)). As a result, training a state-of-the-art DNN model often demands considerable energy, along with the associated financial and environmental costs. For example, a recent report shows that training a single DNN can cost over $10K US dollars and emit as much carbon as five cars in their lifetimes (Strubell et al. (2019)), limiting the rapid development of DNN innovations and raising various environmental concerns.

The recent trends of improving DNN efficiency are mostly focused on compressing models and accelerating inference. An empirically adopted practice is the so-called *progressive pruning and training* routine, i.e., training a large model fully, pruning it and then retraining the pruned model to restore the performance (the process can be iterated several rounds). While this has been a standard practice for model compression (Han et al., 2015), some recent efforts start empirically linking it to the potential of more efficient training. Notably, a latest series of works (Frankle & Carbin, 2019; Liu et al., 2018) reveals that dense, randomly-initialized networks contain small subnetworks which can match the test accuracy of original networks when trained alone themselves. These subnetworks are called *winning tickets*. Despite their insightful findings, there remains to be a major **gap** between the winning ticket observation and the goal of more efficient training, since winning tickets were only identified by pruning unimportant connections in a *fully trained* dense network.

This paper closes this gap by demonstrating the **Early-Bird (EB) tickets** phenomenon: **the winning tickets can be drawn very early in training, and with aggressively low-cost training algorithms**. Through a range of experiments on different DNNs and datasets, we observe the consistent existence of EB tickets, the cheap costs needed to reliably draw them, and develop a novel *mask distance* metric to detect their emergence. After being identified, re-training those EB-tickets (using standard training) leads to comparable or even superior final accuracies, compared to either standard training, or re-training the "ground-truth" winning tickets drawn after full training as in (Frankle & Carbin, 2019). Our observations seem to coincide with the recent findings by (Achille et al., 2019; Li et al., 2019) about the two-stage optimization trajectory in training. Taking advantage of EB tickets, we propose an efficient DNN training scheme termed *EB Train*. To our best knowledge, this is the first step taken towards exploiting winning tickets for a realistic efficient training goal.

Our contribution can be summarized as follow:

1. We discover the Early-Bird (EB) tickets, and show they 1) consistently exist across models and datasets; 2) can emerge very early in training; and 3) stay robust under (and sometimes even favor) various aggressive and low-cost training schemes (in addition to early stopping), including large learning rates and low-precision training.
2. We propose a practical, easy-to-compute mask distance, as an indicator informing to draw EB tickets without accessing the "ground-truth" winning tickets (drawn after full training), fixing a major paradox for connecting winning tickets with the efficient training goal.
3. We design a novel efficient training framework based on EB tickets (EB Train). Experiments in state-of-the-art benchmarks and models show that EB Train can achieve up to **4.7× energy savings**, while maintaining the same or even better accuracy, compared to training with the original winning tickets.

2 Related work

Winning Ticket Hypothesis. The lottery ticket hypothesis (Frankle & Carbin, 2019) first points out that a small subnetwork, called the winning ticket, can be identified by pruning a full trained dense network; when training it in isolation with the same weight initialization once assigned to the corresponding weights in the dense network, one can restore the comparable test accuracy to the dense network. However, finding winning tickets hinged on costly (iterative) pruning and re-training (Morcos et al., 2019) studies the reuse of winning tickets, transferable across different datasets. (Zhou et al., 2019) discovers the existence of supermasks that can be applied to an untrained, randomly-initialized network. (Liu et al., 2018) argues that the weight initialization might make less difference when trained with a large learning rate, while the searched connectivity is more of the winning ticket's core value. It also explores the usage of both unstructured and (more hardware-friendly) structured pruning and shows that both lead to the emergence of winning tickets.

Another related work (Lee et al., 2019) prunes a network at single-shot with one mini-batch, in which the irrelevant connections are identified by a connection sensitivity criterion. Comparing to (Frankle & Carbin, 2019), the authors showed their method to be more efficient in finding the good subnetwork (not the winning ticket), although its re-training accuracy/efficiency was found to be inferior, compared to training the "ground truth" winning ticket.

Other Relevant Observations in Training. (Rahaman et al., 2019; Xu et al., 2019) argue that deep networks will first learn low-complexity (lower-frequency) functional components, before absorbing high-frequency features: the former being more robust to perturbations. An important hint can be found in (Achille et al., 2019): the early stage of training seems to first discover the important connections and the connectivity patterns between layers, which becomes relatively fixed in the latter training stage. That seems to imply that the critical sub-network (connectivity) can be identified independent of, and seemingly also ahead of, the (final best) weights. Finally, Li et al. (2019) demonstrates that training a deep network with a large initial learning rate helps the model focus on memorizing easier-to-fit, more generalizable pattern faster and better – a direct inspiration for us to try drawing EB tickets using large learning rates.

Efficient Inference and Training. Model compression has been extensively studied for lighter-weight inference. Popular means include pruning (Li et al., 2017; Liu et al., 2017; He et al., 2018; Wen et al., 2016; Luo et al., 2017), weight factorization (Denton et al., 2014), weight sharing (Wu

et al., 2018a), quantization (Hubara et al., 2017), and lately network architecture search (Zoph & Le, 2017). On the other hand, the literature on efficient training appears to be much sparser. A handful of works (Goyal et al., 2017; Cho et al., 2017; You et al., 2018; Akiba et al., 2017; Jia et al., 2018; Gupta et al., 2015) focus on reducing the total training time in paralleled, communication-efficient distributed settings. In contrast, our goal is to shrink the total resource cost for in-situ, resource-constrained training. (Banner et al., 2018; Wang et al., 2018) presented low-precision training, which is aligned with our goal and can be incorporated into EB Train (see later).

3 Drawing Early-bird Tickets: Hypothesis and Experiments

We hypothesize that the **winning tickets can emerge at a very early training stage**, which we term as an early-bird (EB) ticket. Consider a dense, randomly-initialized network $f(x;\theta)$, f reaches a minimum validation loss f_{loss} at the i-th iteration with a test accuracy f_{acc}, when optimized with stochastic gradient descent (SGD) on a training set. In addition, consider subnetworks $f(x; m \odot \theta)$ with a mask $m \in \{0, 1\}$ indicates the pruned and unpruned connections in $f(x;\theta)$. When being optimized with SGD on the same training set, $f(x; m \odot \theta)$ reach a minimum validation loss f'_{loss} at the i'-th iteration with a test accuracy f'_{acc}. The EB tickets hypothesis articulates that there exists m such that $f'_{\text{acc}} \approx f_{\text{acc}}$ (even $\geq$), i.e., same or better generalization, with $i' \ll i$ (e.g., early stopping) and sparse m (i.e., much reduced parameters).

Section 3 addresses **three key questions** pertaining to the EB ticket hypothesis. We first show via an extensive set of experiments, that EB tickets can be observed across popular models and datasets (Section 3.1). We then try to be more aggressive to see if high-quality EB tickets still emerge under "cheaper" training (Section 3.2). We finally reveal that EB tickets can be identified with comparing a novel *mask distance* between consecutive epochs, thus no full training needed (Section 3.3).

3.1 Do Early-bird Tickets Always Exist?

We perform ablation simulations using two representative deep models: VGG16 (Simonyan & Zisserman, 2014) and pre-activation residual networks-101 (PreResNet101) (He et al., 2016b), on two popular datasets: CIFAR-10 and CIFAR-100. For drawing the tickets (submodels), we adopt a standard training protocol for both CIFAR-10 and CIFAR-100: the training takes 160 epochs in total and the batch size to 256; the initial learning rate is set to 0.1, and is divided by 10 at the 80th and 120th epochs respectively; the SGD solver is adopted with a momentum of 0.9 and a weight decay of 10^{-4}. For retraining the tickets, we keep the same setting by default.

We follow the main idea of (Frankle & Carbin, 2019), but instead prune networks trained at earlier points (before the accuracies reach their final top values), to see if reliable tickets can still be drawn. We adopt the same channel pruning in (Liu et al., 2017) for all experiments since it is hardware friendly and aligns with our end goal of efficient training (Wen et al., 2016). Fig. 1 reports the accuracies achieved by re-training the tickets drawn from different early epochs. All results consistently endorse that there exist high-quality tickets, at as early as epoch 20 (w.r.t. totally 160 epochs), that can achieve strong re-training accuracies. Comparing among different pruning ratios p, it is not too surprising to see over-pruning (e.g., p = 70%) makes drawing good tickets harder, indicating a balance that we need to calibrate between accuracy and training efficiency.

Two more striking observations from Fig. 1: 1) there consistently exist EB tickets drawn at certain early epoch ranges, that outperform those drawn in later stages, including the "ground-truth" winning tickets drawn at epoch 160. That intriguing phenomenon implies the possible "over-cooking" when networks try to identify connectivity patterns first (Achille et al., 2019), that might hamper generation; 2) some EB tickets are able to outperform even their unpruned, fully-trained models (e.g., the dashlines), potentially thanks to the sparse regularization learned by EB tickets.

3.2 Do Early-bird Tickets Still Emerge under Lower-Cost Training?

For EB tickets, only the important connections found by them (connectivity) matters, while the weights are to be re-trained anyway. One might hence come up with an idea, that more aggressive and "cheaper" training methods might be applicable to further shrink the cost of finding EB tickets (which already implies early stopping of training), as long as the same significant connections still emerge. We experimentally investigate the impacts of two schemes: using appropriate large learning rates, and training in lower precision: EB tickets are observed to survive well under them both.

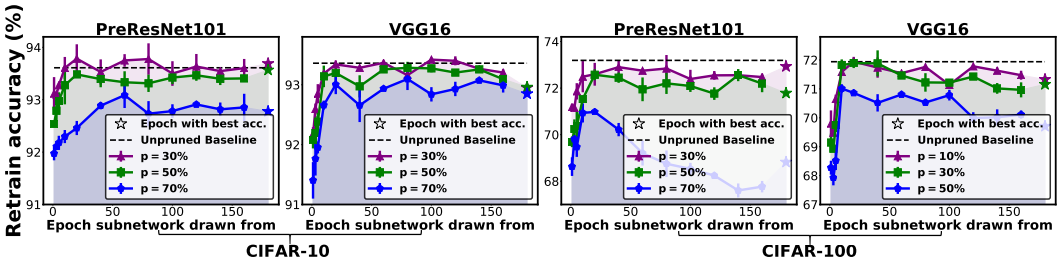

Figure 1: Retraining accuracy vs. epoch number at which the subnetworks are drawn, for both PreResNet101 and VGG16 on CIFAR-10/100 datasets, where p indicates the channel pruning ratio and the dashed line shows the accuracy of the corresponding dense model on the same dataset.

Table 1: The retraining accuracy of subnetworks drawn at different training epochs using different learning rate schedules, where the pruning ratio is 0.5. Here [0, 100] represents $[0_{LR\to 0.01}, 100_{LR\to 0.001}]$ while [80, 120] denotes $[80_{LR\to 0.01}, 120_{LR\to 0.001}]$, for compactness.

	LR Schedule	Retrain acc.(%) (CIFAR-100)				Retrain acc.(%) (CIFAR-10)			
		10	20	40	final	10	20	40	final
VGG16	[0, 100]	66.70	67.15	66.96	69.72	92.88	93.03	92.80	92.64
	[80, 120]	**71.11**	**71.07**	**69.14**	**69.74**	**93.26**	**93.34**	**93.20**	**92.96**
PreResNet101	[0, 100]	69.68	69.69	69.79	70.96	92.41	92.72	92.42	93.05
	[80, 120]	**71.58**	**72.67**	**72.67**	**71.52**	**93.60**	**93.46**	**93.56**	**93.42**

Appropriate large learning rates are important the emergence of EB tickets. We first vary the learning rate schedule in the above experiments. The original schedule is denoted as $[80_{LR\to 0.01}, 120_{LR\to 0.001}]$, i.e., starting at 0.1, decayed to 0.01 at epoch 80, and further decayed to 0.001 at epoch 120. In comparison, we test a new learning rate schedule $[0_{LR\to 0.01}, 100_{LR\to 0.001}]$: starting at 0.01 (epoch 0), and decayed to 0.001 at epoch 100. After drawing tickets, we re-train them all using the same learning rate schedule $[80_{LR\to 0.01}, 120_{LR\to 0.001}]$ for sufficient training and fair comparison. We see from Table 1 that high-quality EB tickets always emerge earlier when searching with the larger $[80_{LR\to 0.01}, 120_{LR\to 0.001}]$ schedule, whose final accuracies are also better. Note that the earlier emergence of good EB tickets contributes to lowering the training costs. It has already been observed that larger learning rates are beneficial for training the dense model fully to draw the winning tickets (Frankle & Carbin, 2019; Liu et al., 2018): we show this benefit extends to EB tickets too. More experiments with larger learning rates can be found in Appendix A.2.

Low-precision training does not destroy EB tickets. We next examine the emergence of EB tickets within a state-of-the-art low-precision training algorithm (Wu et al., 2018b) , where both model weights, activations, gradients and errors are quantized to 8 bits throughout training. Note that we

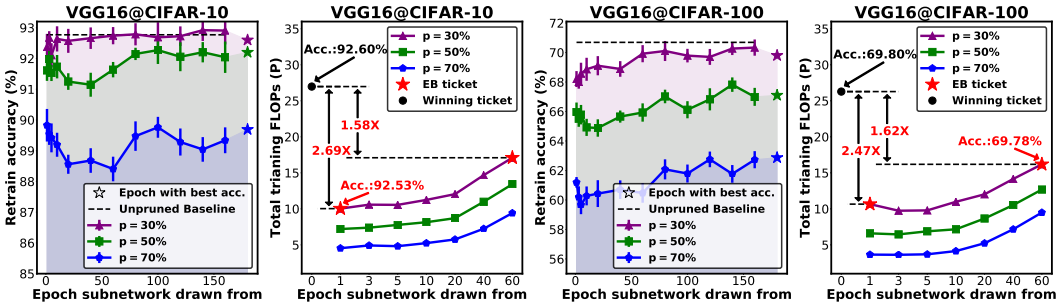

Figure 2: Retraining accuracy and total training FLOPs comparison vs. epoch number at which the subnetworks are drawn, when using 8-bit precision during the stage of identifying EB tickets based on the VGG16 model and CIFAR-10/100 datasets, where p indicates the channel pruning ratio and the dashed line shows the accuracy of the corresponding dense model on the same dataset.

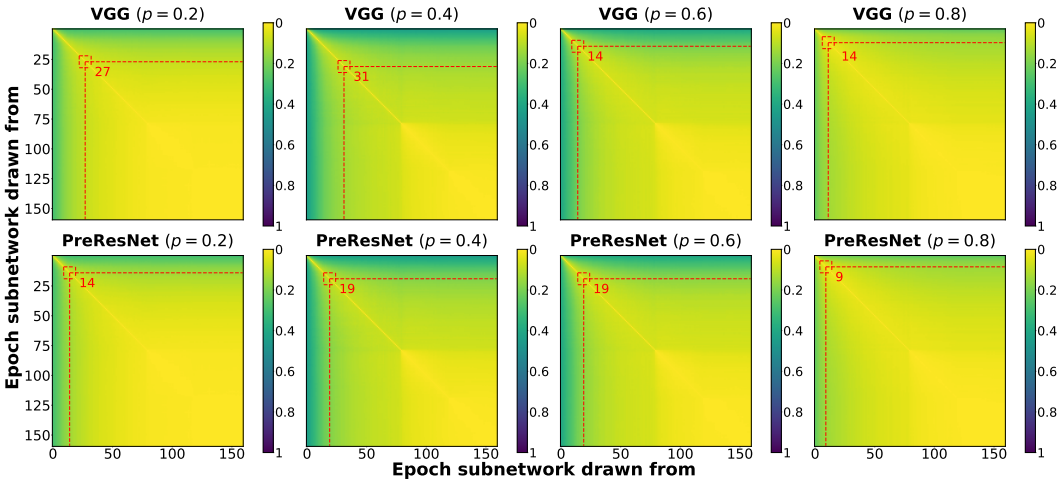

Figure 3: Pairwise mask distance matrix visualization for VGG16 and PreResNet101 on CIFAR100.

only apply low-precision training to the stage of identifying EB tickets, and afterwards the tickets are trained in the same full-precision as in Section 3.1. Fig. 2 shows the retraining accuracy and total number of FLOPs (EB ticket search (8 bits) + retraining (32 bits floating points)) for VGG16 and CIFAR-10/100. We can see that EB tickets still emerge when using aggressively low-precision for identifying EB tickets: the general trends resemble the full-precision training cases in Fig. 1, except the emergence of good EB tickets seem to become even earlier up to initial epochs. In this way, it will lead to cost savings in finding EB tickets, since low-precision updates can aggressively save energy compared to full precision, as in the Tab. 2

3.3 How to Identify Early-Bird Tickets Practically?

Distance between Ticket Masks. For each time of pruning, we define a binary mask of the drawn ticket (pruned subnetwork) w.r.t. the full dense network. We follow (Liu et al., 2017) to consider the scaling factor r in batch normalization (BN) layers as indicators of the corresponding channels' significance. Given a target pruning ratio p, we then prune the channels with top p-percentage smallest r values. Denote the pruned channels as 0 while the kept ones as 1, the original network can be mapped into a binary "ticket mask". For any two sub-networks pruned from the same dense model, we calculate their *mask distance* via the Hamming distance between their two ticket masks.

Detecting EB Tickets via Mask Distances. We first visualize and observe the global behaviors of mask distances between consecutive epochs. Fig. 3 plots the *pairwise mask distance matrices* (160×160) of the VGG16 and PreResNet101 experiments on CIFAR100 (from Section 3.1), at different pruning ratios p, where (i, j)-th element in a matrix denotes the mask distance between epochs i and j in that corresponding experiment (160 epochs in total for all). For the ease of visualization, all elements in a matrix are linearly normalized between 0 and 1; Therefore in the resulting matrix, a lower value (close to 0) indicates a smaller mask distance and is colored warmer (same hereinafter).

Fig. 3 demonstrates fairly consistent behaviors. Taking VGG16 on CIFAR100 ($p = 0.2$) for example: 1) in the beginning, the mask distances change rapidly between epochs, manifested by the quickly "cooling" colors (yellow $\rightarrow$ green), from the diagonal line (lowest since that is comparing an epoch's mask with itself), to off-diagonal (comparing different epochs; the more an element deviates from the diagonal, the more distant the two epochs are away from each other); 2) after 10 epochs, the off-diagonal elements become "yellow" too, and the color transition becomes much smoother from diagonal to off-diagonal, indicating the masks change only very mildly after passing this point; 3) after 80 epochs, the mask distances almost see no change across epochs. Similar trends are observed in other plots too. It seems to concur the hypothesis in (Achille et al., 2019) that a network first learns important connectivity patterns and then fixs them to tune weights more.

Our observation that the ticket masks quickly become stable and hardly changed in early training stages supports drawing EB tickets. We therefore measure the mask distance consecutive epochs, and draw EB tickets when such distance is smaller than a threshold ϵ. Practically, to improve the reliability of EB tickets, we will stop to draw EB tickets when the last five recorded mask distances

are all smaller than ϵ, to avoid some irregular fluctuation in early training stages. In Fig. 3, the red lines indicate the identification of EB tickets when ϵ is set to 0.1.

4 Efficient Training via Early Bird Tickets

In this section, we present an efficient DNN training scheme which leverages the existence of EB tickets and the proposed mask distance that can detect the emergence of EB tickets for time- and energy-efficient training: we call it EB Train. We will first provide a conceptual overview, and then describe the routine of EB Train, and finally show the evaluation performance of EB Train by benchmarking it with state-of-the-art methods of obtaining compressed DNN models based on representative datasets and DNNs.

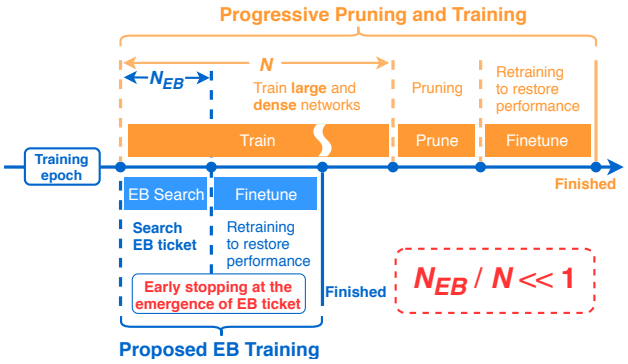

Figure 4: A high-level overview of the difference between EB Train and existing *progressive pruning and training*.

4.1 Why is EB Train More Efficient?

EB Train vs. *Progressive Pruning and Training*. Fig. 4 illustrates an overview of our proposed EB Train and the *progressive pruning and training* scheme, e.g., as in (Frankle & Carbin, 2019). In particular, the *progressive pruning and training* scheme adopts a three-step routine of 1) training a large and dense model, 2) pruning it and 3) then retraining the pruned model to restore performance, and these three steps can be iterated (Han et al., 2015). The first step often dominates (e.g., 75% when using the PreResNet101 model and CIFAR-10 dataset) in terms of training energy and time costs as it involves training a large and dense model. The key feature of our EB Train scheme is that it replaces the aforementioned steps 1 and 2 with a lower-cost step of detecting the EB tickets, i.e., enabling early stopping during the time- and energy-dominant step of training the large and dense model, thus promising large savings in both training time and energy. For example, assuming the first step of the *progressive pruning and training* scheme requires N epochs to sufficiently train the model for achieving the target accuracy, the proposed EB Train needs only N_{EB} epochs to identify the EB tickets making use of the mask distance that can detect the emergence of EB tickets, where $N_{EB} \ll N$ (e.g., $N_{EB}/N = 12.5\%$ in the experiments summarized in Fig.1 and $N_{EB}/N = 6.25\%$ in the experiment summarized in Table 1).

Algorithm 1: EB Ticket Searching Algorithm

Initialize the weights $\boldsymbol{W}$, scaling factor r, pruning ratio p, and the FIFO queue Q with lenght l;
while t (iteration) $< t_{max}$ **do**
  Update $\boldsymbol{W}$ and r using SGD training;
  Perform structured pruning based on r_t towards the target ratio p;
  Calculate the **mask distance** between the current and last subnetworks and add to Q.
  $t = t + 1$
  if Max$(Q) < \epsilon$ **then**
    $t^* = t$
    Return $f(x; m_{t^*} \odot \boldsymbol{W})$ (EB Ticket);
  end if
end while

4.2 How to Implement EB Train?

From Fig. 1, we can see that the EB Train scheme consists of a training (searching) step to identify EB tickets and a fine-tuning step to retrain the EB tickets for achieving the target accuracy. As the fine-tuning step is the same as that of the *progressive pruning and training* baseline, we here only elaborate the first step of searching EB tickets as summarized in *Algorithm* 1. Specifically, the EB searching process 1) first initializes the weights and scaling factors $\boldsymbol{W}$ and $\mathbf{r}$; 2) iterates

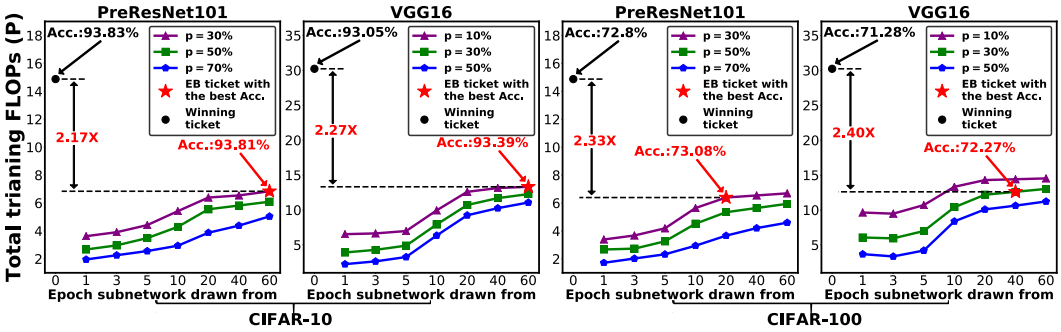

Figure 5: The total number of FLOPs vs. the epoch at which the subnetworks are drawn, for both the PreResNet and VGG16 models on the CIFAR-10 and CIFAR-100 datasets, where p indicates the channel-wise pruning ratio for extracting the subnetworks. Note that the EB tickets at all cases achieve a higher accuracy and consume less computational FLOPs than those of the "ground-truth" winning tickets (drawn after the full training of 160 epochs).

the structured pruning process as in (Liu et al. (2017)) to calculate the mask distances between the consecutive resulting subnetworks, storing them into a first-in-first-out (FIFO) queue of maximum length $l = 5$; and 3) exits when the maximum mask distance in the FIFO is smaller than a specified threshold ϵ (default 0.1 with the [0,1] normalized distances). The output is the resulting EB ticket denoted as $f(x; m_{t^*} \odot \boldsymbol{W})$, which will be retrained further to reach the target accuracy.

While low-precision ticket search has already been proven to be completely feasible and favorable (see Fig. 2), we **do NOT** include it into current efficient training experiments. That is to purposely avoid the over-complicacy that other training algorithms can also be implemented in the same low precision regimes. We do, however, note that EB Train can further aggressively shrink its computation/energy costs, without sacrificing accuracy, by adopting the low-precision ticket search described in Section 3.2. We leave this for the promising next-step work. In the following experiments, both EB Train and its competitors use **32-bit** floating point implementations to ensure fairness.

4.3 How does EB Train Compare to State-of-the-art Techniques?

Experiment Setting. We consider training VGG16 and PreResNet101 models on both CIFAR-10/100 and ImageNet datasets. We measure the training *energy costs from real-device operations:* as the energy cost consists of both computational and data movement costs, the latter of which is often dominant but can not captured by the commonly used metrics, such as the number of FLOPs (Chen et al., 2017), we evaluate the proposed techniques against the baselines in terms of accuracy and real measured energy consumption. Specifically, all the energy consumption of full precision models are obtained by training the corresponding models in an embedded GPU (NVIDIA JETSON TX2). The GPU measurement setup can be found in the Appendix. Note that the energy measurement results include the overhead of using the mask distance to detect the emergence of EB tickets, which is found negligible as compared to the total training cost. For example, for the VGG16 model, the overhead caused by computing mask distances is $\leq 0.029\%$ in memory storage size, $\leq 0.026\%$ in FLOPs, and $\leq 0.07\%$ in real-measured energy costs. This is because 1) the mask distance evaluation only involves simple Hamming distance calculations and 2) each epoch only calculates the distance once.

Results and Analysis. We first compare the computational savings (total number of FLOPs) with the baseline using a *progressive pruning and training* scheme (Liu et al., 2017), when drawing subnetworks at different epochs. Fig. 5 summarizes the results of the PreResNet/VGG16 models and CIFAR-10/100 datasets, corresponding to the same set of experiments as in Fig. 1. We see that EB Train can achieve $\mathbf{2.2} - \mathbf{2.4}\times$ **FLOPs reduction** compared to the common baseline, while leading to comparable or even better accuracy (- 0.81% $\sim$ + 2.38% over the baseline).

Table 2 compares the retraining accuracy and consumed FLOPs/energy of EB Train with four state-of-the-art *progressive pruning and training* techniques: the original lottery ticket (LT) training (Frankle & Carbin, 2019), network slimming (NS) (Liu et al., 2017), ThiNet (Luo et al., 2017) and SNIP (Lee et al., 2019). While all of them involve the process of training a dense network, pruning it, and retraining, they apply different pruning criteria, e.g., NS imposes L_1-sparsity on channel-wise scaling factors from BN layers, and ThiNet greedily prunes the channel that has the smallest effect on the next layers activation values. For EB Train, we by default follow (Liu et al., 2017) to inherit the

Table 2: Comparing the accuracy and energy/FLOPs of EB Train (including its variant), NS (Liu et al. (2017)), LT (Frankle & Carbin, 2019), SNIP (Lee et al., 2019) and ThiNet (Luo et al. (2017)).

Setting	Methods	Retrain acc.			Energy cost (KJ)/FLOPs (x0.05P)		
		p=30%	p=50%	p=70%	p=30%	p=50%	p=70%
PreResNet -101 CIFAR-10	LT (one-shot)	93.70	93.21	**92.78**	6322/298	6322/298	6322/298
	SNIP	93.76	93.31	92.76	3161/148	3161/148	3161/148
	NS	93.83	93.42	92.49	5270/278	4641/254	4211/220
	ThiNet	93.39	93.07	91.42	3579/264	2656/211	1901/173
	EB Train (re-init)	93.88	93.29	92.39	2817/155	2382/141	1565/75.4
	EB Train	**93.91**	**93.90**	92.49	2370/130	1970/114	1452/69.9
	EB Train (LF)	93.48	93.31	92.24	2265/130	1667/102	1338/64.7
	EB Train (LL)	93.24	92.85	92.12	**489.4/130**	**410.9/102**	**281.8/64.7**
	EB Train Improv.	**0.08**	**0.48**	-0.29	**6.5×/1.1×**	**6.5×/1.5×**	**6.7×/2.3×**
VGG16 CIFAR-10	LT (one-shot)	93.18	93.25	**93.28**	746.2/605	746.2/605	746.2/605
	SNIP	93.20	92.71	92.30	373.1/302	373.1/302	373.1/302
	NS	93.05	92.96	92.70	617.1/547	590.7/514	553.8/475
	ThiNet	92.82	91.92	90.40	298.0/451	383.9/379	380.1/331
	EB Train (re-init)	93.11	93.23	92.71	290.4/288	237.3/240	200.5/189
	EB Train	**93.39**	**93.26**	92.71	256.4/**253**	213.4/215	184.2/197
	EB Train (LF)	93.20	93.19	92.91	250.1/261	199.4/214	170.3/164
	EB Train (LL)	93.25	93.13	92.60	**56.1**/261	**43.1/214**	**36.5/164**
	EB Train Improv.	**0.19**	**0.01**	- 0.57	**6.6×/1.2×**	**8.6×/1.4×**	**10.2×/1.8×**
PreResNet -101 CIFAR-100	LT (one-shot)	71.90	71.60	69.95	6095/298	6095/298	6095/298
	SNIP	72.34	71.63	70.01	3047/148	3047/148	3047/148
	NS	72.80	71.52	68.46	4851/274	4310/250	3993/206
	ThiNet	73.10	70.92	67.29	3603/264	2642/211	1893/173
	EB Train (re-init)	73.23	**73.36**	71.05	2413/147	2016/125	1392/70.6
	EB Train	**73.52**	73.15	**72.29**	2020/128	1769/109	1294/65.6
	EB Train (LF)	73.41	73.02	70.72	2038/129	1614/105	1171/59.8
	EB Train (LL)	73.04	71.82	69.45	**434.4/129**	**366.5/105**	**247.3/59.8**
	EB Train Improv.	**0.42**	**1.73**	**2.28**	**7.0×/1.2×**	**7.2×/1.4×**	**7.6×/2.5×**
		p=10%	p=30%	p=50%	p=10%	p=30%	p=50%
VGG16 CIFAR-100	LT (one-shot)	**72.62**	71.31	70.96	741.2/605	741.2/605	741.2/605
	SNIP	71.55	70.83	70.35	370.6/302	370.6/302	370.6/302
	NS	71.24	71.28	69.74	636.5/586	592.3/542	567.8/480
	ThiNet	70.83	69.57	67.22	632.2/547	568.5/451	381.4/379
	EB Train (re-init)	71.65	71.48	69.66	345.3/326	300.0/273	246.8/212
	EB Train	71.81	**72.17**	**71.28**	287.7/282	262.2/**243**	221.7/197
	EB Train (LF)	71.60	71.50	70.27	270.5/277	262.7/252	208.7/194
	EB Train (LL)	71.34	70.53	69.91	**54.6/277**	**64.4**/252	**44.4/194**
	EB Train Improv.	- 0.81	**0.86**	**0.32**	**6.8×/1.1×**	**5.8×/1.2×**	**10.7×/1.6×**

same weight when re-training the searched ticket. We also notice existing debates (Liu et al., 2018) on the initialization re-use, and thus also compare with a variant by re-training the ticket from a new random initialization, termed as *EB Train (re-init)*. Furthermore, we apply the proposed EB Train on top of the low precision training method in (Yang et al., 2019a) and obtain experiment results of another two variants of EB Train: 1) EB Train with low precision search and full precision retrain (i.e., EB Train LF), and 2) EB Train with both low precision search and retrain (i.e., EB Train LL).

Table 2 demonstrates that EB Train consistently outperforms all competitors in terms of saving training energy and computation costs, meanwhile improving the final accuracy in most cases. We use *EB Train Improv.* to record the performance margin (either accuracy, or energy/computation) between EB Train, and the **strongest** competitor among the four state-of-the-art baselines. Specifically, EB Train with full precision floating point (FP32) search and retrain outperforms those pruning methods by up to $\mathbf{1.2-4.7}\times$ and $\mathbf{1.1-4.5}\times$ in terms of the energy consumption and computational FLOPs, while always achieving comparable or even better accuracies, across three pruning ratios, two DNN models and two datasets. Moreover, EB Train with both low precision (8-bits block floating point (FP8)) search and retrain outperforms the baselines by up to $\mathbf{5.8-24.6}\times$ and $\mathbf{1.1-5.0}\times$ in terms of energy consumption estimated using real-measured unit energy from (Yang et al., 2019b) and computational FLOPs. In addition, comparing with the *re-init* variant endorses the effectiveness

Table 3: Compare the accuracy and total training FLOPs of EB Train, Network Slimming (Liu et al., 2017) and SFP (He et al., 2018). The "Acc. Improv" is the accuracy of the pruned model minus that of the unpruned model, so positive number means the pruned model has a higher accuracy.

Methods	Pruning ratio	Top-1 Acc.	Top-1 Acc. Improv. (%)	Top-5 Acc.	Top-5 Acc. Improv. (%)	Total Training FLOPs (P)
Unpruned	-	69.57	-	89.24	-	1259.13
Network Slimming	10%	69.65	+0.08	89.20	-0.04	2424.86
	30%	67.85	-1.72	88.07	-1.17	2168.89
SFP	30%	67.10	-2.47	87.78	-1.46	1991.94
EB Train	10%	**69.84**	**+0.27**	**89.39**	**+0.15**	1177.15
	30%	68.28	-1.29	88.28	-0.96	**952.46**

of initialization inheritance in EB Train. As an additional highlight, EB Train naturally leads to pruned DNN models whose inferences are efficient too, unifying the boost of efficiency throughout the full learning lifecycle.

ResNet18 on ImageNet. To study the performance of EB Train in a harder dataset, we conduct experiments using ResNet18 and ImageNet, and compare its resulting accuracy and total training FLOPs with those of the method in (He et al., 2016a), NS (Liu et al., 2017) and SFP (He et al., 2018) as summarized in Table 3. We can see that 1) when the pruning ratio is 10%, EB Train achieves a better accuracy (+0.27 vs. +0.08 over the unpruned one) while requiring 51% less total training FLOPs, as compared to the NS pruning method; 2) when the pruning ratio is 30%, EB Train results in a higher accuracy (-1.29 vs. -1.72(NS)/-2.47(SFP) over the unpruned one) while reducing the training FLOPs by 56% and 52%, as compared to the NS and SFP baselines. Note that in Table 3, the unpruned results are based on the official implementation in (He et al., 2016a); The SFP results are obtained from their original paper (He et al., 2018), which does not provide results at a 10% pruning ratio; and the NS results are obtained by conducting the experiments ourselves.

5 Discussion and conclusion

We have demonstrated that winning tickets can be drawn at the very early training stage, i.e., EB tickets exist, in both the standard training and several lower-cost training schemes. That motivates a practical success of applying EB tickets to efficient training, whose results compare favorably against state-of-the-arts. Moreover, experiments show that EB Train with low-precision search and retrain achieve more efficient training. We believe many promising problems still remain open to be addressed. An immediate future work is to test low-precision EB Train algorithms on larger models/datasets. We are also curious whether more lower-cost training techniques could be associated with EB tickets. Finally, sometimes high pruning ratios (e.g, $p \geq 0.7$) can hurt the quality of EB tickets and the retrained networks. We look forward to automating the choice of p for different models/datasets, unleashing higher efficiency.

References

Alessandro Achille, Matteo Rovere, and Stefano Soatto. Critical learning periods in deep networks. In *International Conference on Learning Representations*, 2019. URL `https://openreview.net/forum?id=BkeStsCcKQ`.

Takuya Akiba, Shuji Suzuki, and Keisuke Fukuda. Extremely large minibatch sgd: Training resnet-50 on imagenet in 15 minutes. *CoRR*, abs/1711.04325, 2017.

Ron Banner, Itay Hubara, Elad Hoffer, and Daniel Soudry. Scalable methods for 8-bit training of neural networks. In *Advances in Neural Information Processing Systems*, pp. 5145–5153, 2018.

Y. H. Chen, T. Krishna, J. S. Emer, and V. Sze. Eyeriss: An energy-efficient reconfigurable accelerator for deep convolutional neural networks. *IEEE Journal of Solid-State Circuits*, 52(1):127–138, Jan 2017. ISSN 0018-9200.

Minsik Cho, Ulrich Finkler, Sameer Kumar, David S. Kung, Vaibhav Saxena, and Dheeraj Sreedhar. Powerai ddl. *CoRR*, abs/1708.02188, 2017.

Emily L Denton, Wojciech Zaremba, Joan Bruna, Yann LeCun, and Rob Fergus. Exploiting linear structure within convolutional networks for efficient evaluation. In Z. Ghahramani, M. Welling, C. Cortes, N. D. Lawrence, and K. Q. Weinberger (eds.), *Advances in Neural Information Processing Systems 27*, pp. 1269–1277. Curran Associates, Inc., 2014.

Jonathan Frankle and Michael Carbin. The lottery ticket hypothesis: Finding sparse, trainable neural networks. In *International Conference on Learning Representations*, 2019.

Priya Goyal, Piotr Dollár, Ross B. Girshick, Pieter Noordhuis, Lukasz Wesolowski, Aapo Kyrola, Andrew Tulloch, Yangqing Jia, and Kaiming He. Accurate, large minibatch SGD: training imagenet in 1 hour. *CoRR*, abs/1706.02677, 2017. URL `http://arxiv.org/abs/1706.02677`.

Suyog Gupta, Ankur Agrawal, Kailash Gopalakrishnan, and Pritish Narayanan. Deep learning with limited numerical precision. In *International Conference on Machine Learning*, pp. 1737–1746, 2015.

Song Han, Huizi Mao, and William J Dally. Deep compression: Compressing deep neural networks with pruning, trained quantization and huffman coding. *arXiv preprint arXiv:1510.00149*, 2015.

Kaiming He, Xiangyu Zhang, Shaoqing Ren, and Jian Sun. Deep residual learning for image recognition. In *Proceedings of the IEEE conference on computer vision and pattern recognition*, pp. 770–778, 2016a. URL `https://github.com/facebookarchive/fb.resnet.torch`.

Kaiming He, Xiangyu Zhang, Shaoqing Ren, and Jian Sun. Identity mappings in deep residual networks. In *European conference on computer vision*, pp. 630–645. Springer, 2016b.

Yang He, Guoliang Kang, Xuanyi Dong, Yanwei Fu, and Yi Yang. Soft filter pruning for accelerating deep convolutional neural networks. In *International Joint Conference on Artificial Intelligence (IJCAI)*, pp. 2234–2240, 2018.

Itay Hubara, Matthieu Courbariaux, Daniel Soudry, Ran El-Yaniv, and Yoshua Bengio. Quantized neural networks: Training neural networks with low precision weights and activations. *The Journal of Machine Learning Research*, 18(1):6869–6898, 2017.

Xianyan Jia, Shutao Song, Wei He, Yangzihao Wang, Haidong Rong, Feihu Zhou, Liqiang Xie, Zhenyu Guo, Yuanzhou Yang, Liwei Yu, et al. Highly scalable deep learning training system with mixed-precision: Training imagenet in four minutes. *arXiv preprint arXiv:1807.11205*, 2018.

Namhoon Lee, Thalaiyasingam Ajanthan, and Philip HS Torr. Snip: Single-shot network pruning based on connection sensitivity. In *International Conference on Learning Representations*, 2019.

Hao Li, Asim Kadav, Igor Durdanovic, Hanan Samet, and Hans Peter Graf. Pruning filters for efficient convnets. In *International Conference on Learning Representations*, 2017.

Yuanzhi Li, Colin Wei, and Tengyu Ma. Towards explaining the regularization effect of initial large learning rate in training neural networks. *arXiv preprint arXiv:1907.04595*, 2019.

Zhuang Liu, Jianguo Li, Zhiqiang Shen, Gao Huang, Shoumeng Yan, and Changshui Zhang. Learning efficient convolutional networks through network slimming. In *Proceedings of the IEEE International Conference on Computer Vision*, pp. 2736–2744, 2017.

Zhuang Liu, Mingjie Sun, Tinghui Zhou, Gao Huang, and Trevor Darrell. Rethinking the value of network pruning. *arXiv preprint arXiv:1810.05270*, 2018.

Jian-Hao Luo, Jianxin Wu, and Weiyao Lin. Thinet: A filter level pruning method for deep neural network compression. In *Proceedings of the IEEE international conference on computer vision*, pp. 5058–5066, 2017.

Ari S. Morcos, Haonan Yu, Michela Paganini, and Yuandong Tian. One ticket to win them all: generalizing lottery ticket initializations across datasets and optimizers. 2019.

NVIDIA Inc. NVIDIA Jetson TX2. https://www.nvidia.com/en-us/autonomous-machines/embedded-systems/jetson-tx2/, accessed 2019-09-01.

Nasim Rahaman, Aristide Baratin, Devansh Arpit, Felix Draxler, Min Lin, Fred Hamprecht, Yoshua Bengio, and Aaron Courville. On the spectral bias of neural networks. In *Proceedings of the 36th International Conference on Machine Learning*, volume 97 of *Proceedings of Machine Learning Research*, pp. 5301–5310. PMLR, 09–15 Jun 2019.

Karen Simonyan and Andrew Zisserman. Very deep convolutional networks for large-scale image recognition. *arXiv preprint arXiv:1409.1556*, 2014.

Emma Strubell, Ananya Ganesh, and Andrew McCallum. Energy and policy considerations for deep learning in NLP. *CoRR*, abs/1906.02243, 2019. URL http://arxiv.org/abs/1906.02243.

Naigang Wang, Jungwook Choi, Daniel Brand, Chia-Yu Chen, and Kailash Gopalakrishnan. Training deep neural networks with 8-bit floating point numbers. In *Advances in neural information processing systems*, pp. 7675–7684, 2018.

Wei Wen, Chunpeng Wu, Yandan Wang, Yiran Chen, and Hai Li. Learning structured sparsity in deep neural networks. In *Advances in neural information processing systems*, pp. 2074–2082, 2016.

Junru Wu, Yue Wang, Zhenyu Wu, Zhangyang Wang, Ashok Veeraraghavan, and Yingyan Lin. Deep k-means: Re-training and parameter sharing with harder cluster assignments for compressing deep convolutions. *arXiv preprint arXiv:1806.09228*, 2018a.

Shuang Wu, Guoqi Li, Feng Chen, and Luping Shi. Training and inference with integers in deep neural networks. In *International Conference on Learning Representations*, 2018b. URL https://openreview.net/forum?id=HJGXzmspb.

Zhi-Qin John Xu, Yaoyu Zhang, Tao Luo, Yanyang Xiao, and Zheng Ma. Frequency principle: Fourier analysis sheds light on deep neural networks. *arXiv preprint arXiv:1901.06523*, 2019.

Guandao Yang, Tianyi Zhang, Polina Kirichenko, Junwen Bai, Andrew Gordon Wilson, and Christopher De Sa. SWALP : Stochastic weight averaging in low precision training. In *Proceedings of the 36th International Conference on Machine Learning, ICML 2019, 9-15 June 2019, Long Beach, California, USA*, pp. 7015–7024, 2019a. URL http://proceedings.mlr.press/v97/yang19d.html.

Yukuan Yang, Shuang Wu, Lei Deng, Tianyi Yan, Yuan Xie, and Guoqi Li. Training high-performance and large-scale deep neural networks with full 8-bit integers. *arXiv preprint arXiv:1909.02384*, 2019b.

Yang You, Zhao Zhang, Cho-Jui Hsieh, James Demmel, and Kurt Keutzer. Imagenet training in minutes. In *Proceedings of the 47th International Conference on Parallel Processing*, pp. 1. ACM, 2018.

Hattie Zhou, Janice Lan, Rosanne Liu, and Jason Yosinski. Deconstructing lottery tickets: Zeros, signs, and the supermask. In *Advances in Neural Information Processing Systems*, 2019.

Barret Zoph and Quoc V. Le. Neural architecture search with reinforcement learning. In *International Conference on Learning Representations*, 2017. URL https://arxiv.org/abs/1611.01578.

A APPENDIX

A.1 MEASUREMENT OF ENERGY COST

Fig. 6 shows our GPU measurement setup, in which the GPU board is connected to a laptop and a power meter. In particular, the training settings are downloaded from the laptop to the GPU board, and the real-measured energy consumption is obtained via the power meter and runtime measurement for the whole training process.

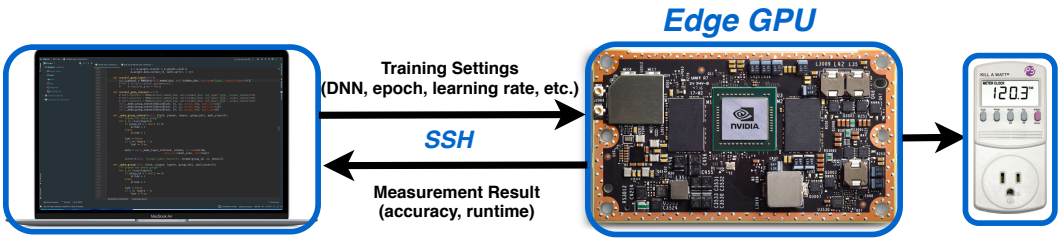

Figure 6: The energy measurement setup (from left to right) with a MAC Air latptop, an embedded GPU (JETSON TX2 (NVIDIA Inc.)), and a power meter.

A.2 APPROPRIATE LARGE LEARNING RATE FAVOR THE EMERGENCE OF EB TICKETS

Here we show the effect of larger learning rates setting. The original schedule is denoted as $[80_{LR\to 0.01}, 120_{LR\to 0.001}]$, i.e., starting at 0.1, decayed to 0.01 at epoch 80, and further decayed to 0.001 at epoch 120. In comparison, we test a larger initial learning rate, staring at 0.5 for VGG16 and starting at 0.2 for PreResNet101. After drawing tickets, we re-train them all using the same learning rate schedule with their searching phase for sufficient training and fair comparison. We see from Table 4 that high-quality EB tickets also emerge early when searching with the larger initial learning rate, whose final accuracies are even better.

Table 4: The retraining accuracy of subnetworks drawn at different training epochs using different inital learning rate, where the pruning ratio is 0.5.

	LR Initial	Retrain acc.(%) (CIFAR-100)				Retrain acc.(%) (CIFAR-10)			
		10	20	40	final	10	20	40	final
VGG16	0.1	**71.11**	71.07	69.14	69.74	93.26	93.34	93.20	92.96
	0.5	70.69	**71.65**	**71.94**	**71.58**	**93.49**	**93.45**	**93.44**	**93.29**
PreResNet101	0.1	71.58	72.67	72.67	71.52	**93.60**	93.46	93.56	93.42
	0.2	**72.58**	**72.90**	**72.86**	**72.71**	93.40	**93.46**	**93.87**	**93.69**